VNU Journal of Science: Mathematics – Physics, Vol. 38, No. 2 (2022) 106-112

VNU Journal of Science: Mathematics - Physics

Journal homepage: https://js.vnu.edu.vn/MaP

Original Article

# Phase Transition in the 2D XY Model with 3-Fold Nematic Interactions

Nguyen Thi Huyen[1], Luu Bich Linh[1], Bui Thi Toan Thu[1], Nguyen Huu Cuong[1], Nguyen Vu Cam Binh[1], Nguyen Thuy Hien[1], Dao Xuan Viet[2], Duong Xuan Nui[1,*]

[1]*Vietnam National University of Forestry, National Road 21, Xuan Mai, Chuong My, Hanoi, Vietnam*

[2]*Advanced Institute for Science and Technology, Hanoi University of Science and Technology, 1 Dai Co Viet, Hai Ba Trung, Hanoi, Viet Nam*

Received 03 December 2021
Revised 22 December 2021; Accepted 22 December 2021

**Abstract:** In this work the results of the study on a generalization of the XY model with an additional $q$-fold nematic-like term through Monte Carlo simulations in two dimensions (2D) have been presented. While the conventional 2D XY model has only integer vortexes, the generalized 2D XY model has both integer and non-integer $1/q$ vortexes, making the phase diagram of the generalized 2D XY model is much richer than that of the conventional 2D XY model. Here, we located the phase transition between the disordered phase (P), the quasi-long-range order phase (F), and the nematic phase (N) for the case of $q = 3$. We provided the numerical evidence to clarify the N−F phase transition of either the first-ordered or second-ordered phase transition. The results showed that the N−F phase transition is the second-ordered, not the first-order phase transition.

*Keywords:* Monte Carlo simulations, phase transitions, magnetic materials.

## 1. Introduction

The generalized 2D XY model is a generalization of the conventional 2D XY model by adding a nematic-like terms. While the standard 2D XY model exhibits only one Kosterlitz Thouless (KT) phase transition between the disordered and quasi-long-range ordered phases, the generalized 2D XY model has a rich phase diagram depending on the relative strength of magnetic and nematic interaction. Some cases of the generalized XY model have been proposed in the interdisciplinary

* Corresponding author.
*E-mail address:* duongxuannui@gmail.com

https//doi.org/10.25073/2588-1124/vnumap.4694

applications for modeling of DNA packing [1] and the structural phases of cyanide polymers [2]. The phase transition of the generalized 2D XY model has been studied by both the theoretical and simulated methods for a long time [3-8].

The Hamilton of the generalized 2D XY model is defined

$$H = J\sum_{<ij>} \Delta cos(\theta_i - \theta_j) + (1-\Delta) cos(q\theta_i - q\theta_j) \quad (1)$$

where $0 \le \theta_i \le 2\pi$ and $q$ is a positive integer ($q$ = 2, 3, 4, ...), $J$ = 1 is the exchange interaction constant. The contribution of magnetic interactions, $\cos(\theta_i - \theta_j)$ and $q$-fold nematic interactions, $\cos(q\theta_i - q\theta_j)$ in Hamiltonian is controlled by $\Delta$ ($0 \le \Delta \le 1$).

For $\Delta$ = 1, one recovers the usual XY model with the KT phase transition. For $\Delta$ = 0, this model is isomorphic to the XY model (by changing variables in the Hamilton, $3\theta_i \rightarrow \theta_i$) with 1/3 KT phase transition. For $0 < \Delta < 1$, this model describes the competition between KT transition (pairs of integer spin vortices with period $2\pi$) and 1/3 KT transition (pair of non-integer spin vortices with period $2\pi/3$) causing three phases. There is a paramagnetic phase (P), a nematic phase (N) and a quasi-long-range ferromagnetic phase (F). While the P−N and P−F transition lines are the KT phase transition [4, 7–9], the N−F line remains controversial. Romano et al. claimed that it is a first-ordered phase transition through mean-field theory [3]. On the other hand, Canova et al. suggested a second-ordered phase transition via Monte Carlo simulation [4, 7]. However, their works have not considered yet direct evidence of a first-ordered phase transition, i.e. the temperature dependence of the energy at the phase transition temperature.

In this work, to further clarify the N−F phase transition is either the first-ordered or the second-ordered, we performed a Monte Carlo simulation for the generalized 2D XY model with $q$ = 3. Several physical quantities, including a magnetic Binder parameter $g_1$, a nematic Binder parameter $g_3$, a temperature derivative of Binder parameter $dg_1/dT$, a temperature derivative of nematic Binder parameter $dg_3/dT$, an energy $E$ and an energy distribution function $P(E)$ are calculated. We will reconstruct the phase diagram of the 2D generalized 2D XY model with $q$ = 3 via the Binder parameters and focus on analyzing the N−F phase transition line.

## 2. Methods

We use Monte Carlo simulation method for the generalized XY model with $q$ = 3 on a square lattice of linear size $L$. The periodic boundary conditions have applied for both axis $x$ and $y$. We use a combination of three algorithms, including the Metropolis algorithm, the Wolff algorithm [10] and the general over-relaxation algorithm [11] to take the system to thermal equilibrium. Equilibrium condition is checked by specific heat calculated through energy fluctuations and temperature difference of energy. Simulation parameters for the systems: The system sizes $L$ = 16, 32, 64 and 128. The total number of Monte Carlo steps $N_{MC} = 6\times10^6$ (where the former half for taking the system to equilibrium, the last half for calculating the physical quantities).

In this work, we calculate several physical quantities as follows. The total energy is defined [12]

$$\langle E \rangle = \frac{1}{2}\left\langle \sum_1^N H_i \right\rangle \quad (2)$$

The magnetic Binder parameter ($g_1$) and the nematic Binder parameter ($g_3$) are defined [12]

$$g = 2 - \frac{\langle m^4 \rangle}{\langle m^2 \rangle^2} \quad (3)$$

with $n$ = 1, 3 and <> denotes thermal average, whereas $m_1$ is the magnetic magnetization and $m_3$ is the nematic magnetization)

$$m = \frac{1}{N}\sqrt{(\sum_{i=1}^{N}\cos(n\theta_i))^2 + (\sum_{i=1}^{N}\sin(n\theta_i))^2} \quad (4)$$

The temperature derivative of magnetic Binder parameter ($dg_1/dT$ ) [13] and nematic Binder parameter ($dg_3/dT$) are:

$$\frac{dg_n}{dT} = \frac{1}{T^2}\left(-\frac{\langle m_n^4 H\rangle}{\langle m_n^2\rangle^2} + \frac{2\langle m_n^4\rangle\langle m_n^2 H\rangle}{\langle m_n^2\rangle^3} - \frac{\langle m_n^4\rangle\langle H\rangle}{\langle m_n^2\rangle^2}\right) \quad (5)$$

## 2. Simulation Results

### *2.1. Phase Diagram*

The $\Delta - T$ phase diagram of the generalized XY model at $q$ = 3 is presented in Figure 1. The phase diagram contains three phases, including the disordered phase (P), the quasi long-range-order phase (F) and the nematic phase (N). The green points are 1/3 KT transition temperature, calculated from the nematic Binder parameter ($dg_3/dT$). The pink points are second-ordered transition temperature as measured by the magnetic Binder parameter $dg_1/dT$. The blue points are KT transition temperature obtained from the magnetic Binder parameter $dg_1/dT$.

For $\Delta$ = 0, this model is isomorphic to the XY model with phase transition temperatures $T_{1/3\mathrm{KT}} \approx 0.893$. For $\Delta$ = 1.0, this model recovers the usual XY model with $T_{\mathrm{KT}} \approx 0.893$. Here, for simplicity, the unit of temperature is considered in the scalar value without $J/k_B$. Thus, to estimate the temperature in Kelvin scalar for materials, $T_{\mathrm{KT}}$ can be calculated from $T_{\mathrm{KT}} \approx 0.893 J/k_B$ ($k_B$ = 1,38.10$^{-23}$J.K$^{-1}$). For example, AgCN has the exchange interaction coupling $J$ = 3.71 kJ.mol$^{-1}$ [1], the phase transition temperature $T_{\mathrm{KT}}$ is found to be of 370 K.

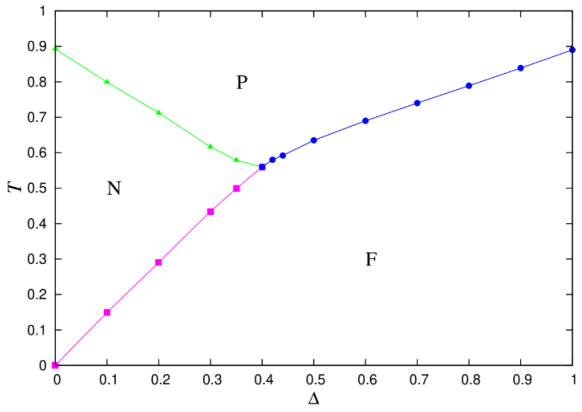


Figure 1. $\Delta - T$ phase diagram of the generalized 2D XY model with $q$ = 3.

In the small $\Delta$ region ($0 < \Delta < 0.4$), Figure 2 presents the temperature dependence of the magnetic Binder parameter ($g_3$) and its temperature derivative ($dg_3/dT$) for $L$=16, 32, 64, 128 at $\Delta$ = 0.2. By increasing size $L$, the magnetic Binder parameter curves increase up to 1 in the low-temperature region, approaching 0 in the high temperature region, and intersect at a temperature (upper inset of

Figure 2a). This behaviour suggests that the phase transition from N phase to F phase is a second-ordered. The temperature derivative of magnetic Binder parameter $dg_1/dT$ has a negative dip at nearly $T_c$. The dip temperature gradually shifts toward $T_c$ by a power law function as $L \to \infty$. $T_c(L)$ is a linear function of $1/L$ (in the inset of Figure 2b), supporting this phase transition is second-ordered.

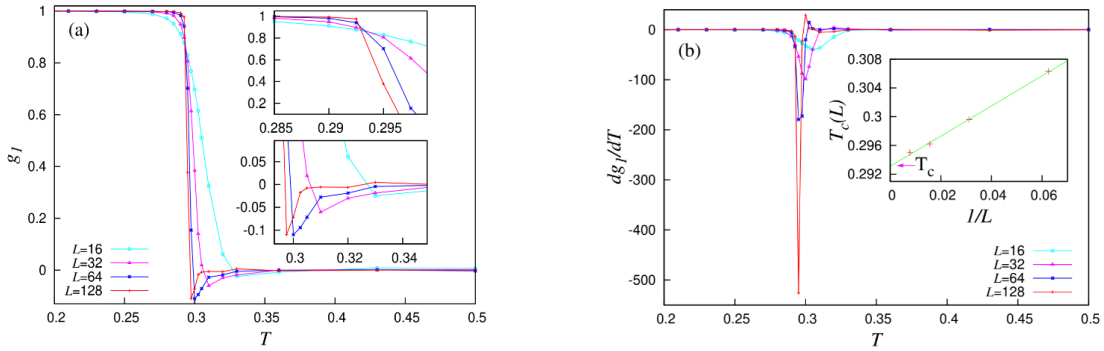


Figure 2. Temperature dependence of the magnetic Binder parameter (a) and the temperature derivative of magnetic Binder parameter (b) in the case $\Delta = 0.2$.

In order to estimate the phase transition temperature, we extrapolate the dip temperature $T_c(L)$ of $dg/dT$ to the thermodynamic limit based on finite-size scaling (FSS) theory. In the case $\Delta = 0.2$, we use the fitting function in Eq. (6) to obtain the phase transition temperature $T_c \approx 0.2932$. This result is consistent with the previous group that calculated $T_c$ from the susceptibility [7] and the correlation length [14].

$$T_C(L) = T_C(\infty) + b.L^{-1/\nu} \quad (6)$$

Figure 3 presents the temperature dependence of the nematic Binder parameter $g_3$ and the derivative of the nematic Binder parameter $dg_3/dT$ at $\Delta = 0.2$ for different lattice sizes. The $g_3$ curves tend to merge in the low-temperature region, and decreases to 0 in the high temperature region (Figure 3a). This behaviour of $g_3$ suggests that the phase transition from P phase to N phase is 1/3KT [15]. $dg_3/dT$ exhibits a negative dip that deepens with increasing system sizes $L$. The dip temperature gradually shifts towards $T_{1/3KT}$ as a logarithmic function.

For $\Delta = 0.2$, in contrast to calculation of $T_c$ from the magnetic Binder parameter, it is not easy to calculate precisely the 1/3 KT phase transition temperatures from $g_3$, so we use the temperature derivative of the nematic Binder parameter, $dg_3/dT$ , to determine the phase transition temperature.

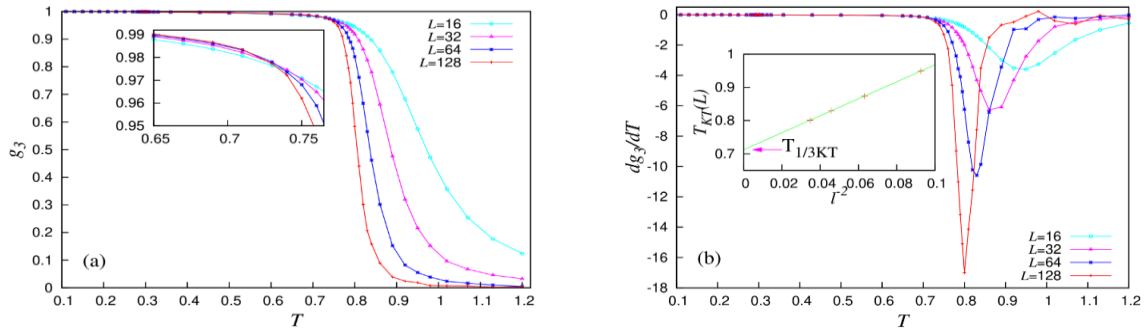


Figure 3. Temperature dependence of the nematic Binder parameter (a) and the temperature derivative of the nematic Binder parameter (b) in the case $\Delta = 0.2$.

We calculate the phase transition temperatures based on Eq. (7) [16], we plot the dip temperature $T_{1/3\mathrm{KT}}(L)$ as a function of $l^{-2}$ (where $l = \ln(bL)$) and determine the fit parameter $b = 1.672$ and the phase transition temperatures $T_{1/3\mathrm{KT}} \approx 0.712$ (inset of Figure 3(b)). This result is consistent with the previous results who calculated $T_c$ from the susceptibility [7] and from the correlation length [14].

$$T_{1/3KT}(L) = T_{1/3KT} + \frac{c^2 T_{1/3KT}}{(\ln(bL))^2} \tag{7}$$

In the large Δ region ($0.40 < \Delta \leq 1.0$), there is no nematic phase. In case $\Delta = 0.7$, the Binder parameter curves tend to merge in low-temperature region and decreases towards 0 in the high-temperature region (Figure 4(b)). This behavior of g suggests P–F phase transition is a KT phase transition. In a similar way as $\Delta = 0.2$, the phase transition temperatures $T_{\mathrm{KT}} \approx 0.734$ are calculated from the $\mathrm{d}g_1/\mathrm{d}T$ (inset of Figure 4b).

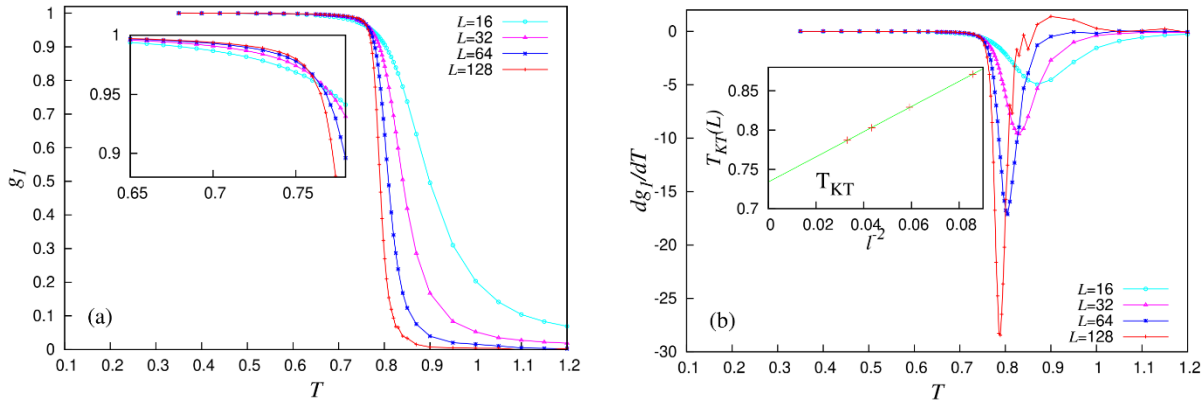


Figure 4. Temperature dependence of the magnetic Binder parameter (a) and the temperature derivative of the magnetic Binder parameter (b) in the case $\Delta = 0.7$.

### *2.2. N − F Phase Transition Line*

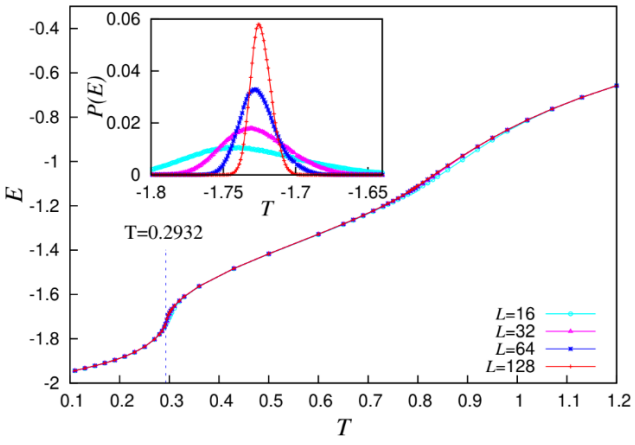


Figure. 5. Temperature dependence of the energy in the case $\Delta = 0.2$. The inset presents the distribution function of energy at a temperature near $T_c$.

This section clarifies that the N−F phase transition (Figure 1) is either a first-ordered phase transition or a second-ordered phase transition. In the N−F line, typical case $\Delta = 0.2$ in the inset of (Figure 2), the magnetic Binder parameter also exhibits a negative dip which deepens for $L$ increasing from 16 to 64 a signal of first-ordered phase transition) [17] and does not deepen for $L$ rising from 64 to 128 (a signal of none first-ordered transition). One more, the temperature dependence of energy also seems to has a jump near $T_c \approx 0.2932$ (a signal of discrete energy) [18] in Figure 5.

In order to distinguished that jump of energy is discrete or continuous, we calculate the distribution function of the energy $P(E)$ at several temperatures nearly $T_c$ for different $\Delta$ along with the N−F line. In the case of $\Delta = 0.2$, the distribution function of energy $P(E)$ at $T = 0.2932$ is shown in the inset of Figure 5. $P(E)$ appears only one peak. In similar way, we also calculate $P(E)$ for many different temperatures around $T_c$, including $T$ = 0.2920; 0.2922; 0.2924; 0.2926; 0.2928; 0.2930; 0.2932; 0.2934; 0.2936; 0.2938; 0.2940; 0.2942; 0.2944; 0.2946; 0.2948; 0.2950. $P(E)$ also exhibits only one peak as in the case of $T = T_c = 0.2932$, suggesting that the N−F phase transition is not a first-ordered. Overall, the behavior of $g$, d$g$/d$T$, and $E$ suggests that the N−F phase transition is a second-ordered. This result is consistent with the previous simulation results [7, 14] and different from the theoretical results of Romano et al. [3] who analyzed the N−F phase transition by using the mean-field theory.

## 3. Conclusion

In this work, we have studied the behaviors of the magnetic and nematic Binder parameter $g_n$, its temperature derivative d$g_n$/d$T$, the energy, and its distribution function in the two-dimensional generalized XY model at $q = 3$. We have reconstructed the phase diagram of this model via the temperature derivative of the magnetic and nematic Binder parameters. We also provided numerical evidence to confirm that the N−F phase transition is the second-ordered, but not the first-order phase transition.

## Acknowledgements

This research is funded by Vietnam National University of Forestry (VNUF) under Grant No. LN.CC-2021.6.

## References

[1] G. M. Grason, Structural Transitions and Soft Modes in Frustrated DNA Crystals, Europhysics Letters,Vol. 83, No. 5, 2008, pp. 580031-580036, https://doi.org/10.1209/0295-5075/83/58003.

[2] A. B. Cairns, M. J. Cliffe, J. A. M. Paddison, D. Daisenberger et al., Encoding Complexity within Supramolecular Analogues of Frustrated Magnets, Nature Chemistry Vol. 8, 2016, pp. 442-447, https://doi.org/10.1038/nchem.2462.

[3] S. Romano, Topological Transitions in Two-Dimensional Lattice Spin Models, Physical Review E, Vol. 73, 2016, pp. 0427011-0427012, https://doi.org/10.1103/PhysRevE.73.042701.

[4] F´. C. Poderoso, J. J. Arenzon, Y. Levin, New Ordered Phases in a Class of Generalized XY Models, Physical Review Letters, Vol. 106, 2011, pp. 0672021-0672024, https://doi.org/10.1103/PhysRevLett.106.067202.

[5] Y. Shi, A. Lamacraft, P. Fendley, Boson Pairing and Unusual Criticality in a Generalized xy Model, Physical Review Letters, Vol. 107, 2011, pp. 2406011-2406015, https://doi.org/10.1103/PhysRevLett.107.240601.

[6] D. M. H¨ubscher, S. Wessel, Stiffness Jump in the Generalized xy Model on the Square Lattice, Physical Review E, Vol. 87, 2013, pp. 0621121-0621125, https://doi.org/10.1103/PhysRevE.87.062112.

[7] G. A. Canova, Y. Levin, J. J. Arenzon, Kosterlitz-Thouless and Potts Transitions in a Generalized XY Model, Physical Review E, Vol. 89, 2014, pp. 0121261-0121265, https://doi.org/10.1103/PhysRevE.89.012126.

[8] G. A. Canova, Y. Levin, J. J. Arenzon, Competing Nematic Interactions in a Generalized xy Model in Two and Three Dimensions, Physical Review E, Vol. 94, 2016, pp. 0321401-03214012, https://doi.org/10.1103/PhysRevE.94.032140.

[9] D. X. Nui, L. Tuan, N. D. T. Kien, P. T. Huy, D. T. Hung, D. X. Viet, Correlation Length in a Generalized Two-Dimensional XY Model, Physical Review B, Vol. 98, 2018, pp. 1444211-1444219, https://doi.org/10.1103/PhysRevB.98.144421.

[10] U. Wolff, Collective Monte Carlo Updating for Spin Systems, Physical Review Letters, Vol. 62, 1989, pp. 361-364, https://doi.org/10.1103/PhysRevLett.62.361.

[11] K. Kanki, D. Loison, and K.D. Schotte, Efficiency of the Microcanonical Over-relaxation Algorithm for Vector Spins Analyzing First and Second Order Transitions, The European Physical Journal B, Vol. 44, 2005, pp. 309-315, https://doi.org/10.1140/epjb/e2005-00130-7.

[12] J. Imriska, Phase Diagram of a Modified XY Model, Bachelor's Thesis, Comenius University in Bratislava, 2009.

[13] C. M. Lapilli, P. Pfeifer, C. Wexler, Universality Away from Critical Points in Two-Dimensional Phase Transitions, Physical Review Letters, Vol. 96, 2006, pp. 1406031-1406034, https://doi.org/10.1103/PhysRevLett.96.140603.

[14] D. X. Nui, Monte Carlo Study of KosterlitzThouless Phase Transition Phenomenon in the Generalized 2D XY Model, Ph.D. Thesis, Hanoi University of Science and Technology, 2020 (in Vietnamese).

[15] M. Nishino, S. Miyashita, Termination of the Berezinskii-Kosterlitz-Thouless Phase with a New Critical Universality in Spin-Crossover Systems, Physical Review B, Vol. 92, 2015, pp. 1844041-1844047, https://doi.org/10.1103/PhysRevB.92.184404.

[16] Y. Komura, Y. Okabe, Large-Scale Monte Carlo Simulation of Two-Dimensional Classical XY Model Using Multiple Gpus, Journal of the Physical Society of Japan, Vol. 81, 2012, pp. 1130011-1130014, https://doi.org/10.1143/JPSJ.81.113001.

[17] R. M. Liu, W. Z. Zhuo, J. Chen et al., Shkin-Teller Criticality and Weak First-Order Behavior of the Phase Transition to a Fourfold Degenerate State in Two-Dimensional Frustrated Ising Antiferromagnets, Physical Review E, Vol. 96, 2017, pp. 0121031-0121037, https://doi.org/10.1103/PhysRevE.96.012103.

[18] S. Sinha, S. K. Roy, Finite Size Scaling and First-Order Phase Transition in a Modified XY Model, Physical Review E, Vol. 81, 2010, pp. 0221021-0221024, https://doi.org/10.1103/PhysRevE.81.022102.